Electronic Supplementary Material (ESI) for New Journal of Chemistry.

Using geometric simulation software 'GASP' to model conformational flexibility in a family of zinc metal-organic frameworks

William J. Gee,[a] Stephen A. Wells,[b] Simon J. Teat,[c] Paul R. Raithby,[d] and Andrew D. Burrows*[d]

a) School of Environment and Science, Griffith University, 170 Kessels Road, Brisbane, QLD 4111, Australia.
b) Department of Chemical Engineering, University of Bath, Claverton Down, Bath, BA2 7AY, United Kingdom
c) Advanced Light Source, Lawrence Berkeley National Laboratory, Berkeley, CA, USA.
d) Department of Chemistry, University of Bath, Claverton Down, Bath, BA2 7AY, United Kingdom. Email: a.d.burrows@bath.ac.uk.

Supporting Information

* To whom correspondence should be addressed.
Email: a.d.burrows@bath.ac.uk Telephone: +44 (0) 1225 386529

Table of Contents

1. Accurate mass spectrometry performed on the reaction mixture post H_3cbt formation

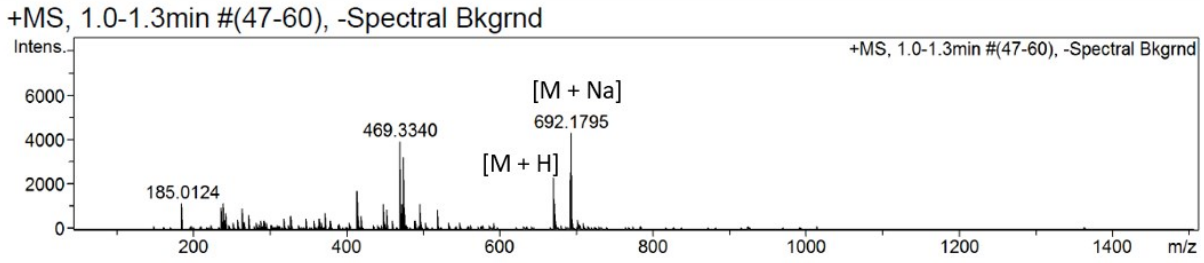

#	m/z	I	I %	Area	S/N	
1	185.0124	1179	27.4	29	3602.7	
2	239.0221	1140	26.5	43	1218.1	
3	413.2697	1705	39.7	56	479.7	
4	469.3340	3937	91.6	155	809.8	
5	472.1151	1113	25.9	82	225.9	[aldol]
6	474.1297	3222	74.9	256	647.8	
7	670.1946	2302	53.5	276	337.5	
8	671.1987	1132	26.3	128	165.0	
9	692.1795	4300	100.0	502	653.6	
10	693.1800	2117	49.2	238	323.6	

Generate Molecular Formula Parameters

Charge	Tolerance	SearchRadius	H/C Ratio min.	H/C Ratio max.	Electron Conf.	Nitrogen Rule	sigma limit
positive	10 ppm	0.05 m/z	0	3	both	true	0.05

Expected Formula C42 H27 N3 O6 **Adduct(s):** H, Na

#	meas. m/z	theo. m/z	Err[ppm]	Sigma	Formula
1	670.1946	670.197811	4.00	0.0248	C 42 H 28 N 3 O 6
1	692.1795	692.179755	-0.50	0.0184	C 42 H 27 N 3 Na 1 O 6

The reaction mixture during H_3**cbt** formation was analysed by mass spectrometry after microwave heating had concluded to assess the oxidation of the dihydropyridine. Both the $[M+H]^+$ and $[M+Na]^+$ ions were present in the crude mixture, as well as trace amounts of aldol product shown below. The peak at 474 m/z can be attributed to reduction of the aldol intermediate to balance oxidation of the dihydropyridine. Imine formation of the aldol carboxylic acids / ketone groups derived from aqueous ammonia could account for the peak at 469 m/z.

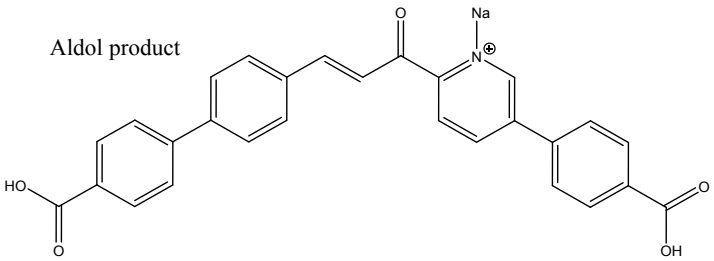

m/z: 472.1155 (100.0%), 473.1189 (30.3%), 474.1223 (2.7%), 474.1223 (1.7%), 474.1198 (1.0%)

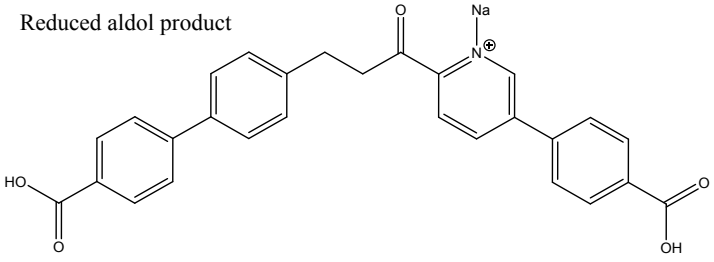

m/z: 474.1312 (100.0%), 475.1345 (30.3%), 476.1379 (2.7%), 476.1379 (1.7%), 476.1354 (1.0%)

2. ^{1}H-NMR spectrum of ligand H_3cbt in DMSO-d_6

Expanded Region of Interest:

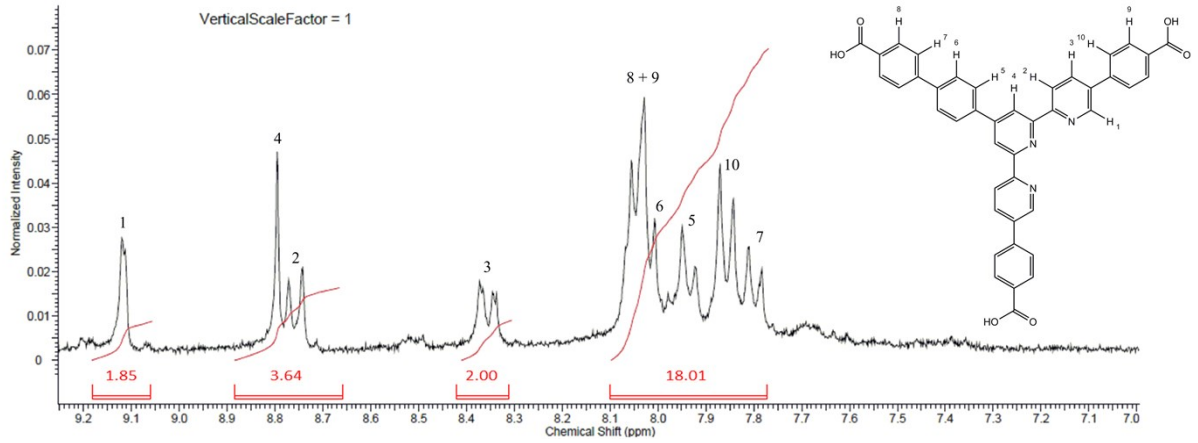

Mid-range view:

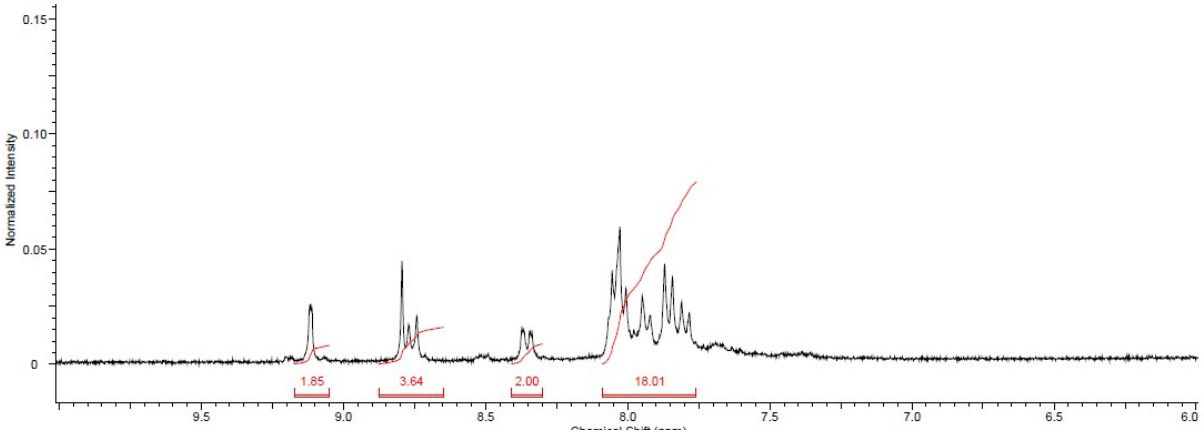

Full Spectrum:

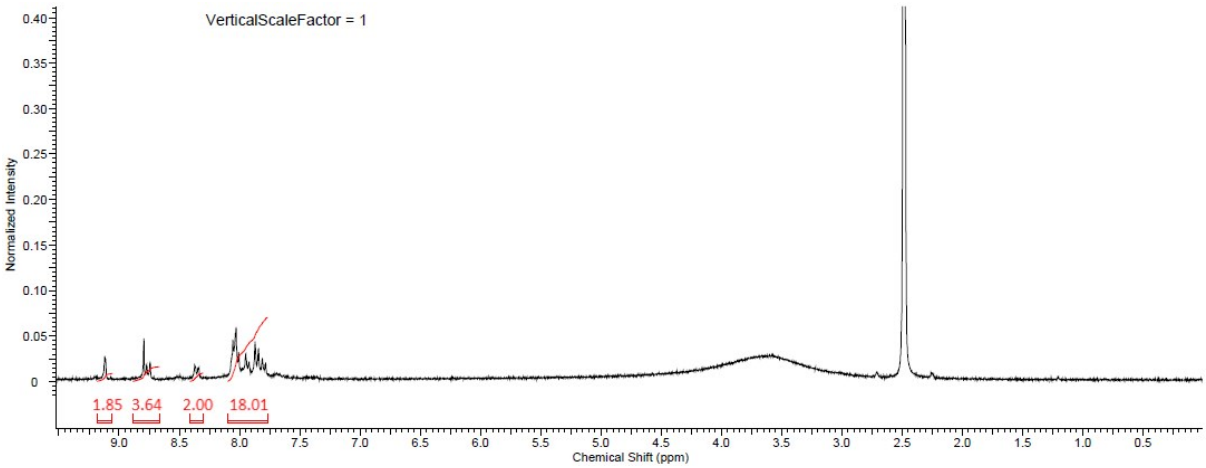

3. Crystal data table for 1–3:

Identification code	**1**	**2**	**3**
Empirical formula	C53 H42 N7 O10 Zn	C106 H100 N8 O25 S8 Zn2	C48 H24 N5 O11 Zn
Formula weight	1002.3	2273.15	912.09
Temperature	150(2) K	150(2) K	150(2) K
Wavelength	0.71073 Å	0.71073 Å	0.71073 Å
Crystal system	Monoclinic	Monoclinic	Monoclinic
Space group	P 21/n	P 21/c	P 21/n
Unit cell dimensions	a = 16.5565(17) Å	a = 15.823(4) Å	a = 17.733(5) Å
	b = 14.5139(15) Å	b = 16.228(5) Å	b = 11.753(3) Å
	c = 21.112(2) Å	c = 22.530(6) Å	c = 22.790(6) Å
	α= 90°.	α= 90°.	α= 90°.
	β= 104.938(2)°.	β= 108.133(4)°.	β= 96.427(4)°.
	γ = 90°.	γ = 90°.	γ = 90°.
Volume	4901.8(9) $Å^3$	5498(3) $Å^3$	4720(2) $Å^3$
Z	4	2	4
Density (calculated)	1.358 Mg/m^3	1.373 Mg/m^3	1.284 Mg/m^3
Absorption coefficient	0.568 mm^{-1}	0.663 mm^{-1}	0.584 mm^{-1}
F(000)	2076	2360	1860
Crystal size	0.2 x 0.2 x 0.1 mm^3	0.3 x 0.2 x 0.2 mm^3	0.4 x 0.2 x 0.2 mm^3
Theta range for data collection	2.503 to 31.676°.	2.657 to 20.729°.	2.666 to 23.308°.
Index ranges	-24<=h<=24, -21<=k<=20, -30<=l<=30	-15<=h<=15, -16<=k<=16, -22<=l<=22	-19<=h<=19, -13<=k<=13, -25<=l<=25
Reflections collected	72286	25904	38697
Independent reflections	15845 [$R_{(int)}$ = 0.0695]	5654 [$R_{(int)}$ = 0.1108]	6786 [$R_{(int)}$ = 0.0559]
Completeness to theta = 25.000°	99.50%	99.30%	99.50%
Absorption correction	Semi-empirical from equivalents	None	Semi-empirical from equivalents
Max. and min. transmission	0.7313 and 0.6864		0.7452 and 0.6517
Refinement method	Full-matrix least-squares on F_2	Full-matrix least-squares on F_2	Full-matrix least-squares on F_2
Data / restraints / parameters	15845 / 5 / 646	5654 / 10 / 629	6786 / 20 / 539
Goodness-of-fit on F_2	1.037	1.047	1.089
Final R indices [I>2sigma(I)]	R_1 = 0.0635, wR_2 = 0.1845	R_1 = 0.1087, wR_2 = 0.2802	R_1 = 0.1037, wR_2 = 0.3004
R indices (all data)	R_1 = 0.0754, wR_2 = 0.1957	R_1 = 0.1583, wR_2 = 0.3224	R_1 = 0.1249, wR_2 = 0.3220
Largest diff. peak and hole	1.535 and -0.717 e.$Å^{-3}$	2.359 and -1.066 e.$Å^{-3}$	1.699 and -0.952 e.$Å^{-3}$

4. H-bonding environment about the nonbonding Hcbt arm in 1-3.

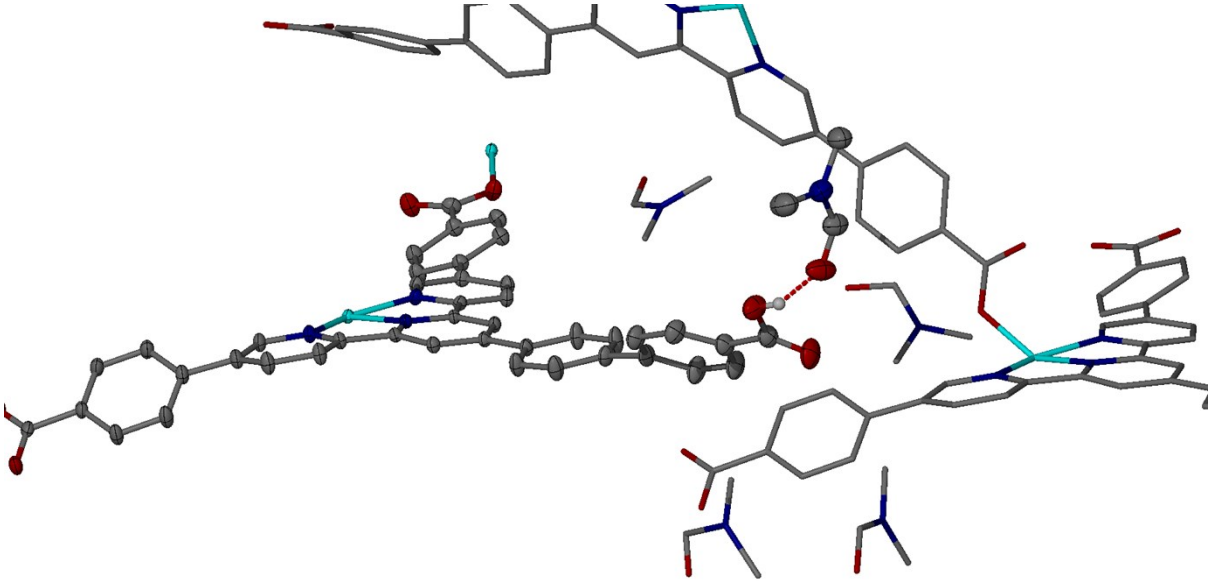

Structure 1: Ligand H-bonding observed in **1** to a molecule of DMF which orders the remaining solvent molecules within the channel. Inter-oxygen hydrogen-bond length is 2.636(3) Å

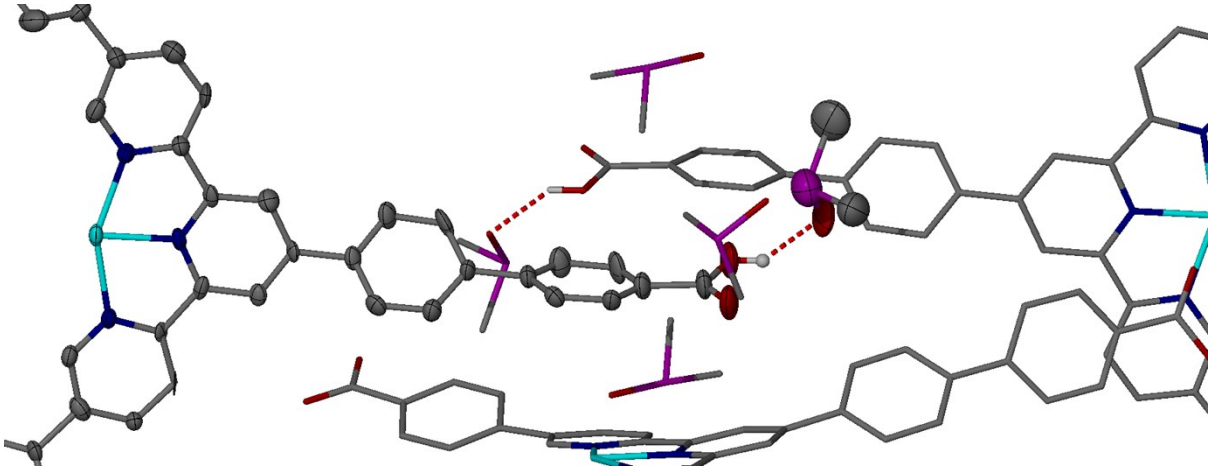

Structure 2: Ligand H-bonding observed in **2** to a molecule of DMSO which orders the remaining solvent molecules within the channel. The inter-oxygen hydrogen-bond length is 2.626(15) Å

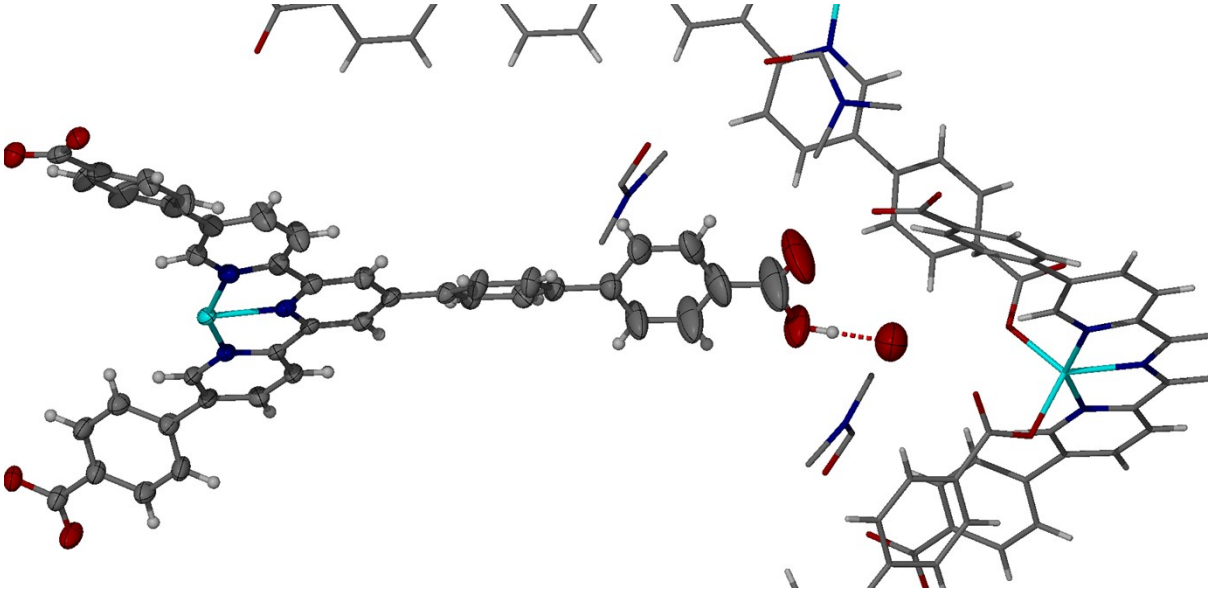

Structure 3: Ligand H-bonding observed in **3** to a water molecule which partially orders the remaining solvent molecules within the channel. The inter-oxygen hydrogen-bond length is 2.616(14) Å

5. TGA traces of 1 and 2.

TGA trace of 1.

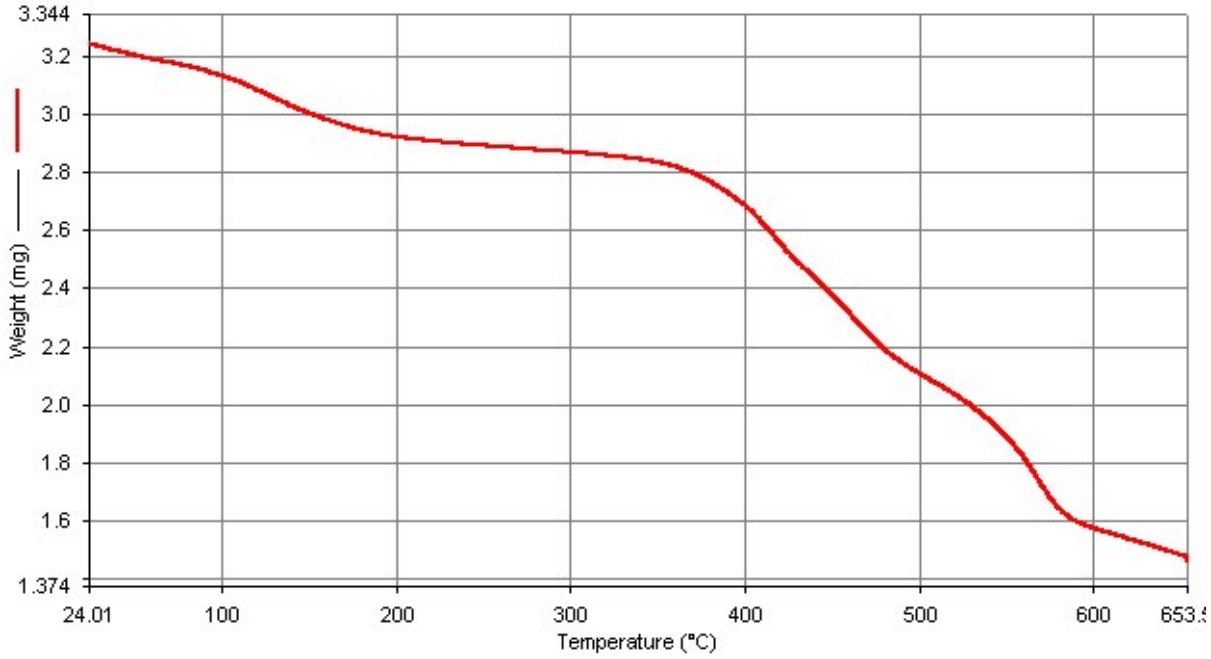

TGA trace of 2.

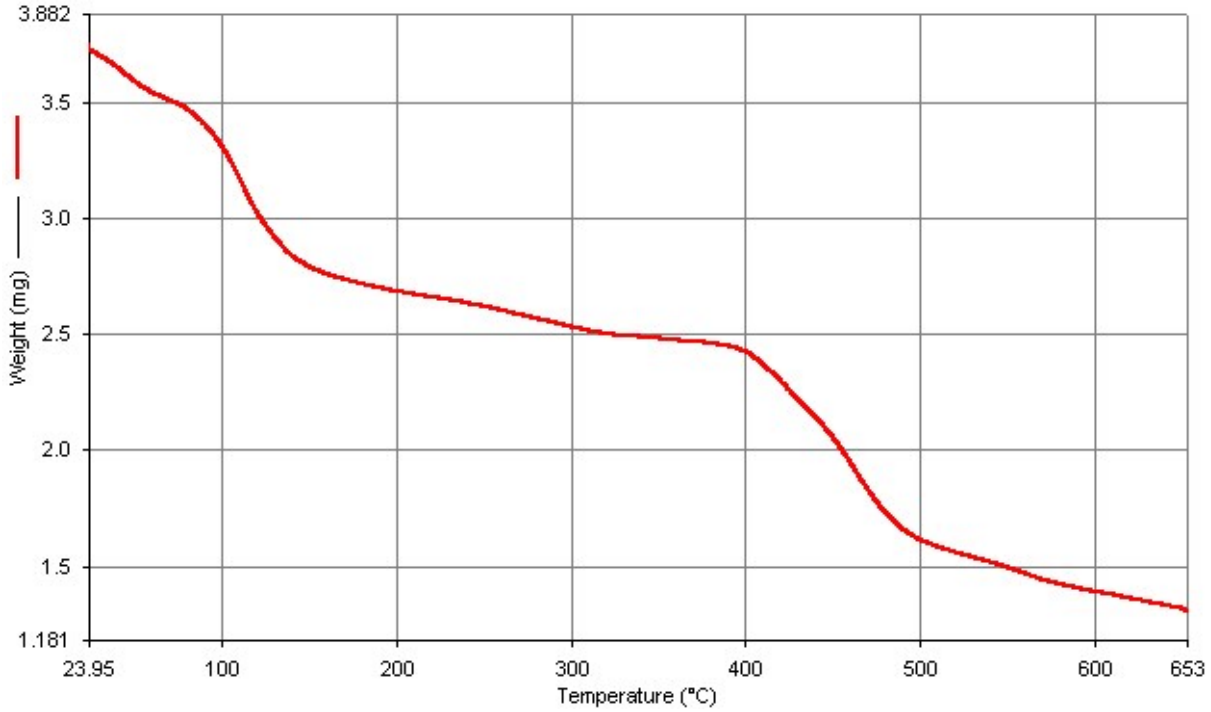

6. PXRD analysis of compounds 1 and 2.

$[Zn(Hcbt)]_n \cdot 4DMF$ (1)

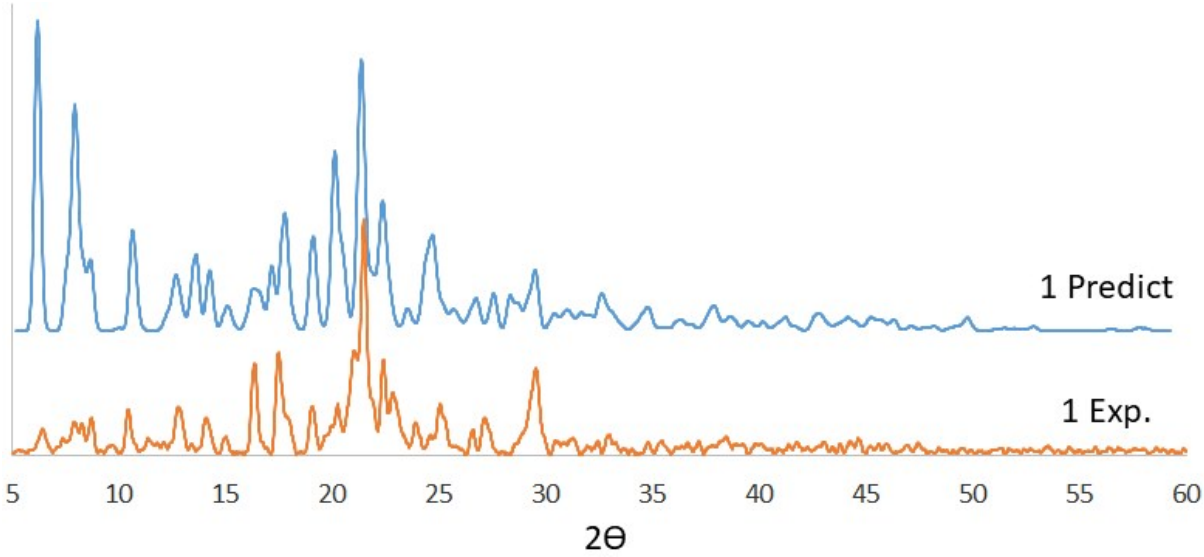

Some minor variation in peak positions, particularly at lower 2Θ values, are likely due to the mismatch between collection temperatures between the powder data (room temp.) and crystal data used for collection (150 K), coupled with the propensity of the material to desolvate triggering changes in conformation (see TGA in S4).

$[Zn(Hcbt)]_n \cdot 4DMSO \cdot 1.5H_2O \cdot DMF$ (2)

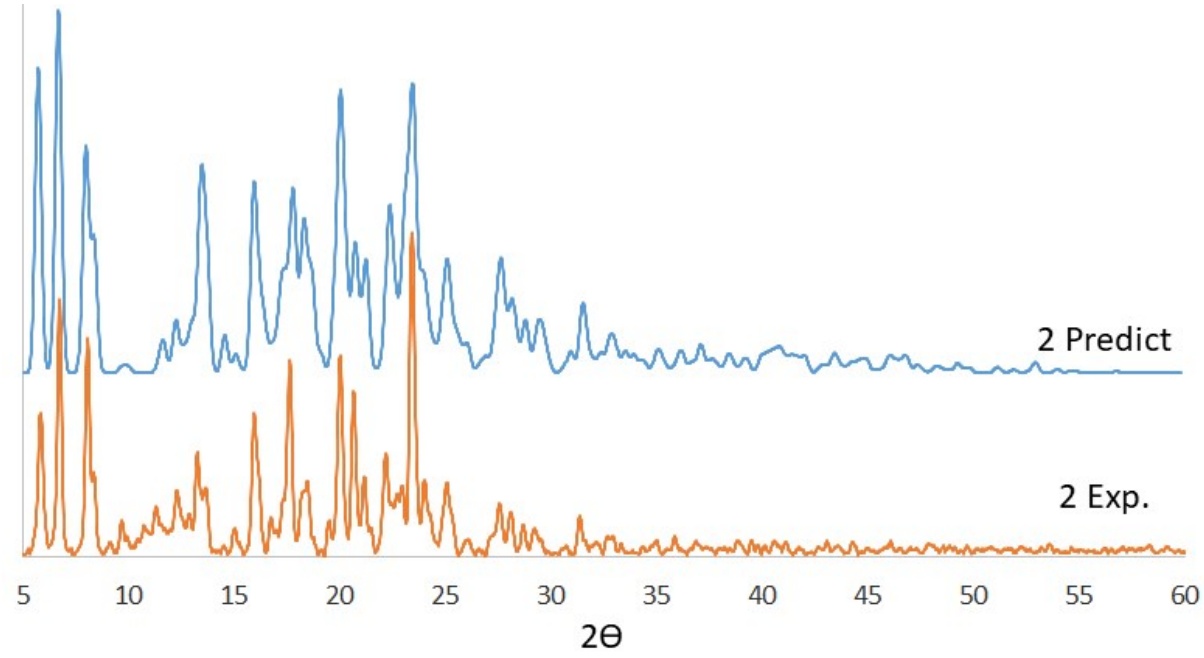

7. Comparison of experimental PXRD pattern of 1 to predicted pattern of 3.

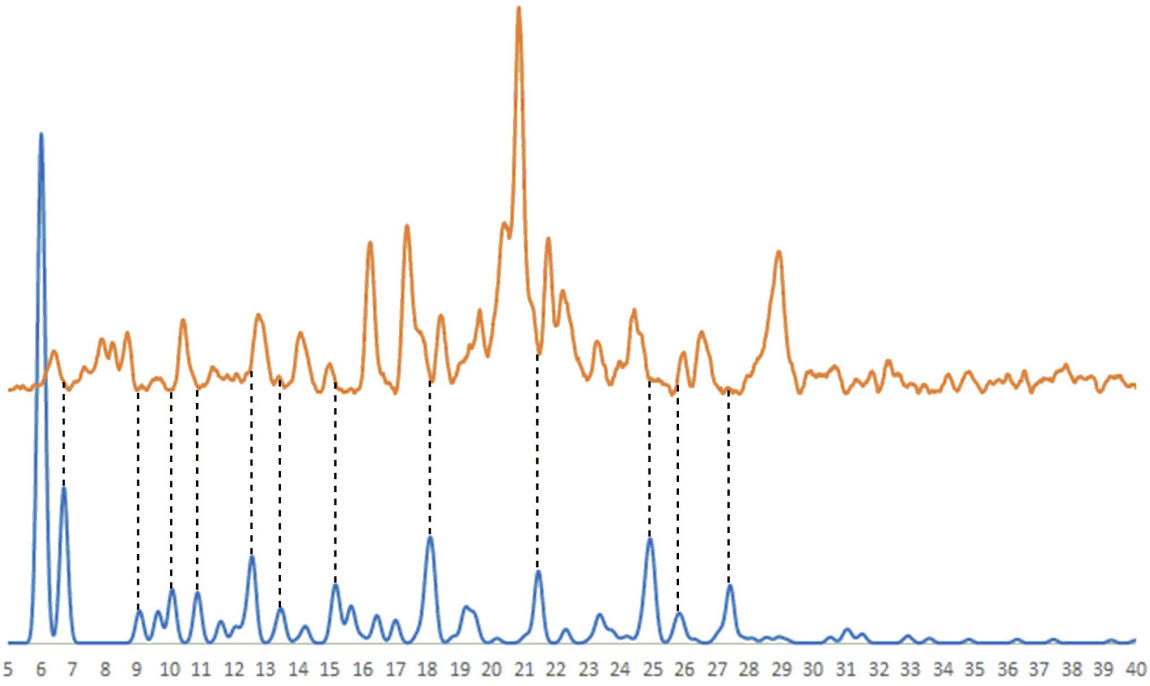

A comparison of the predicted PXRD pattern for **3** (bottom, blue trace) to the experimental PXRD pattern obtained for **1** using dry DMF (top, orange trace). In most instances the peaks for **3** correspond to troughs in **1**, highlighting that a negligible amount of **3** is present within **1** when dry DMF is used during synthesis.

8: Tolerance of 1 to immersion in water for twelve hours.

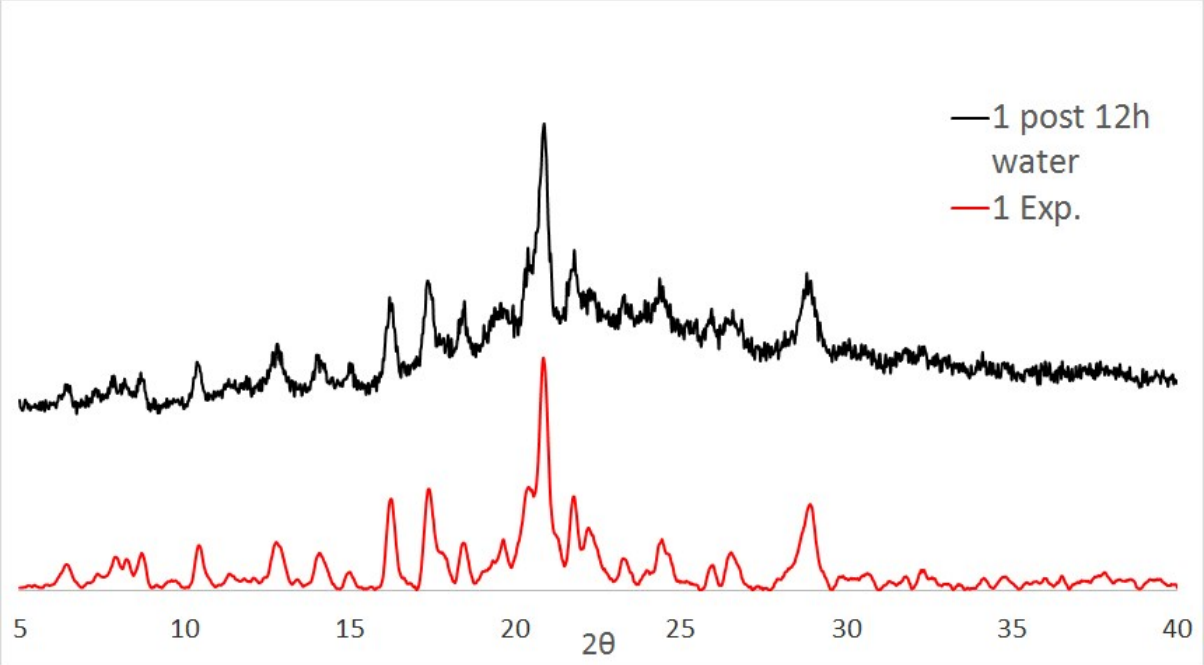

Despite being suspended in water for a period of 12 hours, framework **1** gave no evidence of interconversion to a hydrated motif (*e.g.* **3**). This finding provides experimental validity for a topological barrier preventing interconversion between the neat DMF motif (**1**) and the hydrated motif (**3**) identified by GASP.

9: Influence of activation on frameworks 1 and 2 assessed by PXRD.

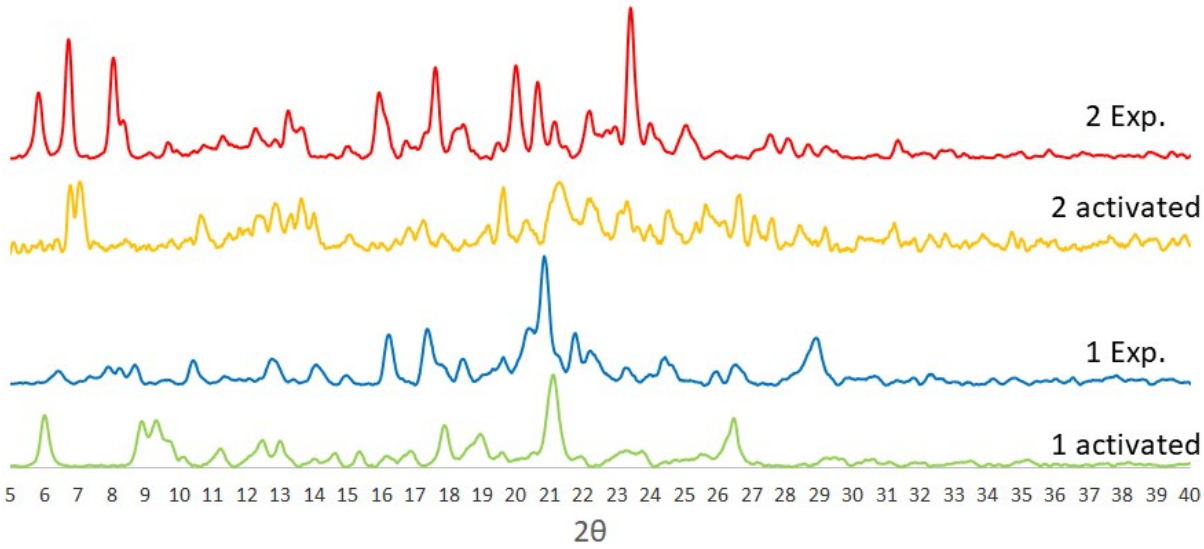

A comparison of how activation (heating at 150 °C under high vacuum for 8 hours) impacted the PXRD pattern of MOFs **1** and **2**. Both structures retain crystallinity upon desolvation, however new PXRD patterns for each were observed. Conformational changes to minimise pore volume as predicted by GASP serve to explain the changes in pattern. It should also be noted that upon activation the two frameworks remain structurally distinct from one another, consistent with GASP inferences of a barrier to interconversion between the two motifs.